

Original Article

Voltage Stability of a Photovoltaic DC Microgrid Using Artificial Neural Network

Kalangiri Manohar¹, Kottala Padma²

^{1,2}Department of Electrical Engineering, Andhra University College of Engineering, Visakhapatnam, India.

¹Corresponding Author : kmanohar@andhrauniversity.edu.in

Received: 14 August 2023

Revised: 16 September 2023

Accepted: 14 October 2023

Published: 31 October 2023

Abstract - This article puts forth a control strategy for a DC microgrid utilizing an Artificial Neural Network (ANN) as the controller. Using the Approximation Dynamic Programming (ADP) technique, the ANN controller is trained with the Levenberg-Marquardt approach; a FATT technique is employed for the resulting Jacobian matrix. To assess the effectiveness of the ANN, power DC converter switching models are utilized. The findings reveal that the suggested controller demonstrates a remarkable ability to maintain voltage stability in a freestanding DC microgrid, which improves over the prior controller. Moreover, the ANN controller exhibits outstanding performance in DC microgrids, as it rapidly responds to voltage references and endures load disruptions in diverse transient conditions. This study emphasizes the efficiency and reliability of the proposed control approach using ANN for regulating DC microgrids, making it a promising solution for future microgrid implementations.

Keywords - PV array, Proportional Integral (PI) controller, Artificial Neural Network controller (ANN), DC-DC converters, ADP.

1. Introduction

The assessment of the security and stability of the photovoltaic DC microgrid system hinges on using the bus voltage as a reference point [1]. However, due to the inherently variable and unpredictable nature of photovoltaic power generation and the dynamic fluctuations in loads, the operation of the PV DC microgrid may result in unforeseen power interruptions, leading to significant variations in bus voltage. Consequently, preserving DC bus voltage stability and maintaining power quality have emerged as critical concerns that demand immediate attention [2].

Presently, Energy Storage Devices (ESDs) are seamlessly integrated into the DC bus via Bidirectional DC/DC Converters (BDCs) to counteract these fluctuations [3, 4]. The micro power source contributes energy, and the load absorbs power based on the load bus's requirements, reinforcing the system's resilience [5]. Incorporating ESDs into the DC bus through BDCs represents a promising approach to sustaining voltage stability and ensuring power quality in photovoltaic DC microgrid systems, offering an efficient and effective method for managing power fluctuations.

Energy storage unit converters predominantly employ a dual closed-loop control strategy that simultaneously regulates voltage and current or an updated variant. In this context, the conventional dual closed-loop voltage and

current control, rooted in classic control theory, utilize the bus voltage as the outermost control layer while internally managing the energy-storing inductive current with a compensatory PI controller [6]. Although this conventional control approach enhances the system's dynamic response, it falls short of effectively mitigating substantial fluctuations and the influence of DC bus voltage.

Consequently, there is a pressing need for alternative control methodologies to address these limitations and enhance the stability and dependability of energy storage unit converters. More sophisticated and advanced control algorithms, including adaptive and predictive control strategies, emerge as potential solutions to overcome these challenges and elevate the performance of energy storage unit converters across diverse operational conditions.

To address this challenge, various researchers have embraced a methodology that combines the conventional dual closed-loop control with the feedforward control technique [7]. Depending on the variables employed in the feedforward approach, these strategies can be classified into power feedforward and current feedforward techniques. For example, three load current feedforward control strategies were devised to target the unstable zero point of the boost converter. These strategies proved more effective than feedback control in curtailing voltage fluctuations and improving system stability, particularly when reducing the



output filter capacitance [8]. Furthermore, Hou et al. integrated load current feedforward into the control loop through direct power control. Experimental and simulation outcomes demonstrated a significant enhancement in the dynamic response of DC converters and the ability to maintain a constant output voltage even in the face of abrupt load changes.

Additionally, Lu et al. introduced the incorporation of a ripple compensation link through load current feedforward to lessen the quality of systematic output power and expedite the response time of the existing inner loop control. While the current feedforward control approach described above enhances the system's dynamic response, it still contends with the issue of voltage and current loop delays, resulting in a slower response of the output current to load disturbances.

The power feedforward control approach is deployed to mitigate fluctuations in bus voltage by injecting disturbance power into the control path [9]. A power feedforward compensation control strategy, employing classical dual closed-loop control, is applied to tackle the challenge of bus voltage fluctuations resulting from disparities between output power and renewable energy load consumption within the microgrid. This strategy directs power disturbances into the controller through the feedforward channel, effectively curtailing bus voltage fluctuations and enhancing overall system stability [10].

Furthermore, Song and Zhu introduced a practical, direct power control strategy associated with direct power feedforward control to bolster the bidirectional DC/DC converter's resilience against load disturbances. This method prevents the need to account for the converter's energy storage inductance and varying transformer ratio parameters, thereby enhancing overall system compatibility [11].

Additionally, power feedforward aids in hastening the system's response to power disturbances, consequently improving its ability to regulate bus voltage fluctuations to some extent. It is worth noting that power feedforward, akin to current feedforward, must traverse the inner loop, delaying the output current response to load disturbances.

Moreover, it is essential to acknowledge that feedforward control necessitates real-time monitoring of system parameters, which may increase system costs and reduce reliability. This aspect is not conducive to expanding the microgrid or the widespread adoption of plug-and-play capabilities. To address the challenges associated with feedforward control, utilising a state observer eliminates the need for a precise mathematical model encompassing the disturbance signal when assessing the disturbance magnitude. This approach simplifies model development, circumvents intricate mathematical computations, and satisfies the real-time requirements of the system. However,

deploying an observer to monitor the system's state variables introduces noise, albeit within the context of relatively straightforward models.

This study attempts to tackle the challenges of time variability and nonlinearity within PV-based microgrids [12]. The proposed approach involves replacing the traditional dual closed-loop control with an Artificial Neural Network (ANN) [13] controller. The ANN controller demonstrates superior transient performance when substantial bus voltage fluctuations occur. Conversely, a PI controller achieves strong steady-state performance when bus voltage variations are modest.

The results obtained from both simulations and experiments affirm that both ANN and PI controllers offer a range of benefits, including rapid response, minimal overshoot, high resilience, and robust anti-jamming capabilities across diverse operating conditions. This investigation underscores the potential of ANN controllers in augmenting the performance and stability of photovoltaic DC microgrids.

2. Description of the Microgrid System

The microgrid being analyzed in this study operates at a voltage level of 48 volts, depicted in Figure 1. In island mode, the power balance is maintained by controlling the distributed energy sources and compensating devices. The microgrid comprises three DC buses, each linked to its corresponding subsystem and governed by a Regional Controller (RC). Loads are connected to each bus and distributed throughout the system.

2.1. About Photovoltaic (PV) System

The PV system is linked to the bus and is subjected to variations in temperature and irradiance. It is equipped with battery storage. A boost converter is employed for Maximum Power Point Tracking (MPPT) to optimise the array's power output. This converter utilizes the Incremental Conductance (InC) approach and an additional integral regulator to ensure robustness. Advanced MPPT techniques may be employed when necessary.

By the InC method, at the MPPT, the derivative of Module power is presumed to be zero, positive to the left of the Maximum Power Point (MPP), and negative to the right of the MPP [14]. The search for the applied PV voltage utilizing the InC technique concludes when the system's InC and system conductance are equivalent, corresponding to the point of lowest rate of change in PV Power (P_{pv}).

This can be mathematically represented.

$$\frac{dP_{PV}}{dP_{PV}} \approx 0 \quad (1)$$

Substituting for $P_{pv} = V_{pv} I_{pv}$ in (1)

$$\frac{dI_{pv}}{dV_{pv}} = -\frac{I_{pv}}{V_{pv}} \tag{5}$$

$$\frac{d((V_{pv})(I_{pv}))}{dV_{pv}} \approx 0 \tag{2}$$

$$I_{pv} \frac{dV_{pv}}{dV_{pv}} + V_{pv} \frac{dI_{pv}}{dV_{pv}} \approx 0 \tag{3}$$

$$I_{pv} + V_{pv} \frac{dI_{pv}}{dV_{pv}} \approx 0 \tag{4}$$

Based on the InC algorithm, the DC-DC converter is responsible for adjusting the operational point of the PV array to satisfy Equation (5). The battery regulates the bus voltage, which runs its converter in constant voltage mode. Consequently, the converter can operate in Continuous Current Mode (CCM), delivering the microgrid with the maximum achievable power output. Any surplus energy generated is stored in the battery storage, enabling the PV system to operate in MPPT mode continuously.

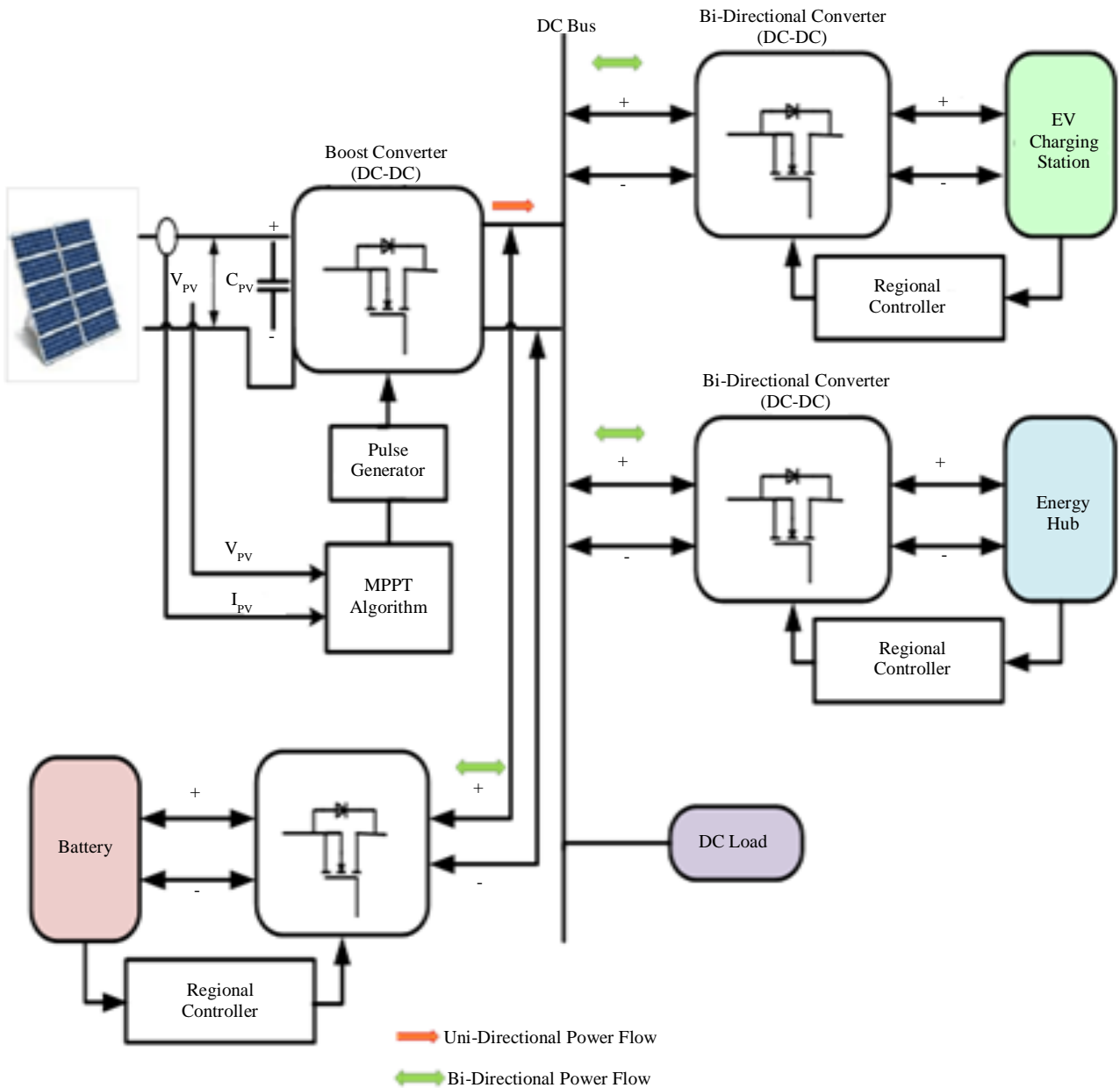


Fig. 1 Solar PV based DC microgrid System

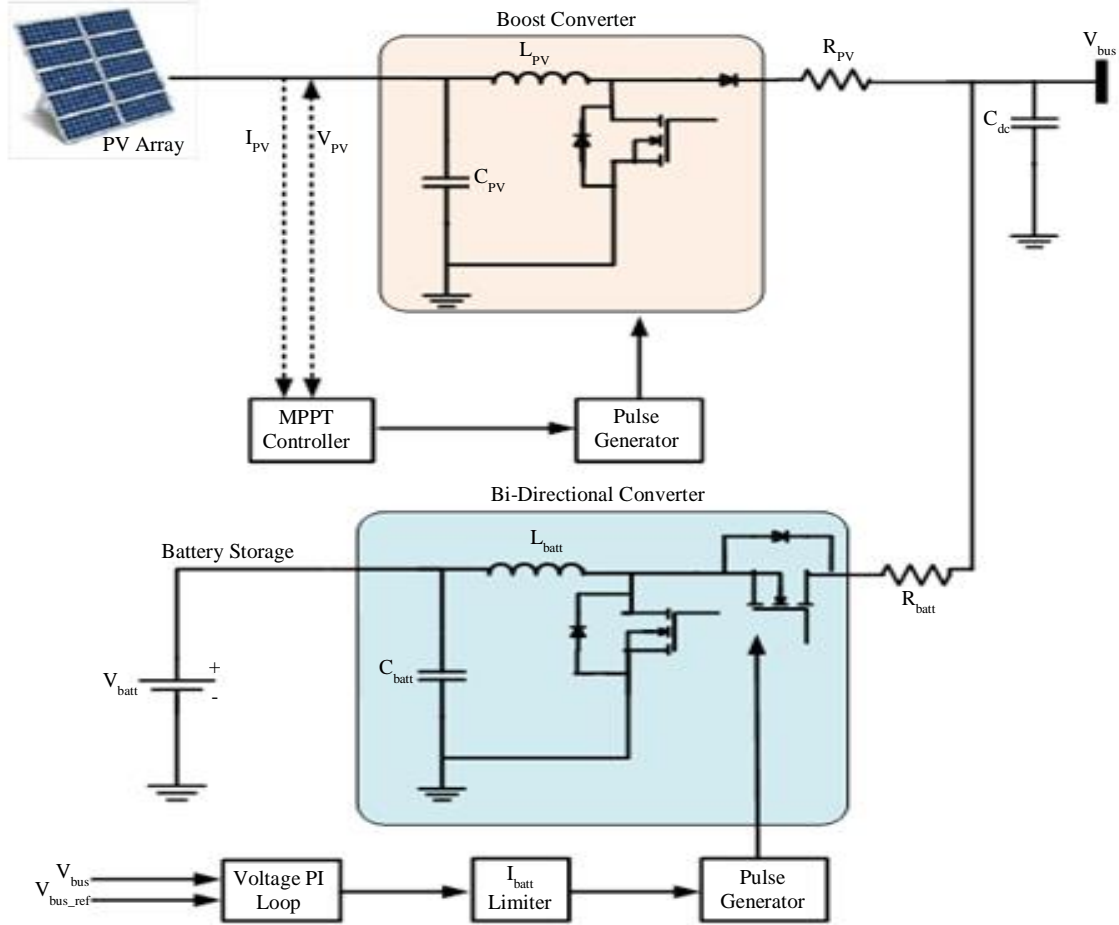


Fig. 2 Implemented PV-battery system

Figure 2 provides a comprehensive illustration of the subsystem. The PV panel's unidirectional converter operates in MPPT mode, while the battery's bidirectional converter employs a Proportional-Integral (PI) controller to regulate the bus voltage.

Surplus power within the microgrid is utilized to charge the battery storage, and the charging current is carefully managed to uphold a consistent bus voltage.

2.2. Bidirectional DC/DC Converter

DC-DC power converters are crucial components of DC microgrid systems because they convert electricity from various voltage levels to the appropriate output voltage. Traditional DC converters, on the other hand, only handle unidirectional power transfer, limiting bidirectional power flow. To circumvent this constraint, the suggested solution employs bidirectional converters, as shown in Figure 3, to enable the charging and discharging of storage devices like batteries and supercapacitors.

This streamlines the process and allows more effective use of the stored energy, making the system more adaptable and robust. The converter's dynamic model includes parasitic

resistances, designated as R_L and R_C , to specify the characteristics of the inductor and capacitor, respectively. The converter's state-space model is expressed as Equations (6) and (7), where the system matrices are denoted as A , B , C and D .

$$x' = Ax + Bu \tag{6}$$

$$y = Cx + Du \tag{7}$$

The converter's State-Space Model (SSM) may be acquired by taking the average of two discrete SSMs. The first SSM is related to the case when M_1 is ON and M_2 is OFF for a duty cycle of d_1 , as shown in Equation (8). The second SSM corresponds to the case when M_1 is OFF, and M_2 is ON for a duty cycle d_2 , equal to 1 minus d_1 , as shown in Equation (9). The state variables chosen are i_L and V_c , represented by x_1 and x_2 , respectively.

$$x'_{d1} = \begin{pmatrix} \frac{-R_L}{L} & 0 \\ 0 & \frac{-1}{C(R + R_C)} \end{pmatrix} x + \begin{pmatrix} \frac{1}{L} \\ 0 \end{pmatrix} u \tag{8}$$

$$x'_{d2} = \begin{pmatrix} \frac{1}{L} \left(R_L + \frac{RR_C}{R+R_C} \right) & \frac{-1}{L} \left(1 + \frac{R_C}{R+R_C} \right) \\ \frac{R}{C(R+R_C)} & \frac{-1}{C(R+R_C)} \end{pmatrix} x + \begin{pmatrix} \frac{1}{L} \\ 0 \end{pmatrix} u \quad (9)$$

Equations (10) and (11) can be utilized to derive the averaged State-Space Model (SSM), resulting in Equation (12).

$$A = d_1 A_1 + d_2 A_2 \quad (10)$$

$$B = d_1 B_1 + d_2 B_2 \quad (11)$$

$$\begin{pmatrix} \frac{1}{L} \left(R_L (1-2d) + \frac{RR_C}{R+R_C} d' \right) & \frac{-1}{L} \left(1 + \frac{R_C}{R+R_C} \right) d' \\ \frac{R(1-d)}{C(R+R_C)} & \frac{-1}{C(R+R_C)} \end{pmatrix} x + \begin{pmatrix} \frac{1}{L} \\ 0 \end{pmatrix} u \quad (12)$$

Similarly, the matrices C & D can be derived, resulting in Equation (13) as shown below.

$$y = \begin{pmatrix} 1 & 0 \\ 0 & 1 \end{pmatrix} x + \begin{pmatrix} \frac{1}{L} \\ 0 \end{pmatrix} u \quad (13)$$

The obtained averaged SSM depicts the converter's performance throughout a complete cycle with a period of T_s .

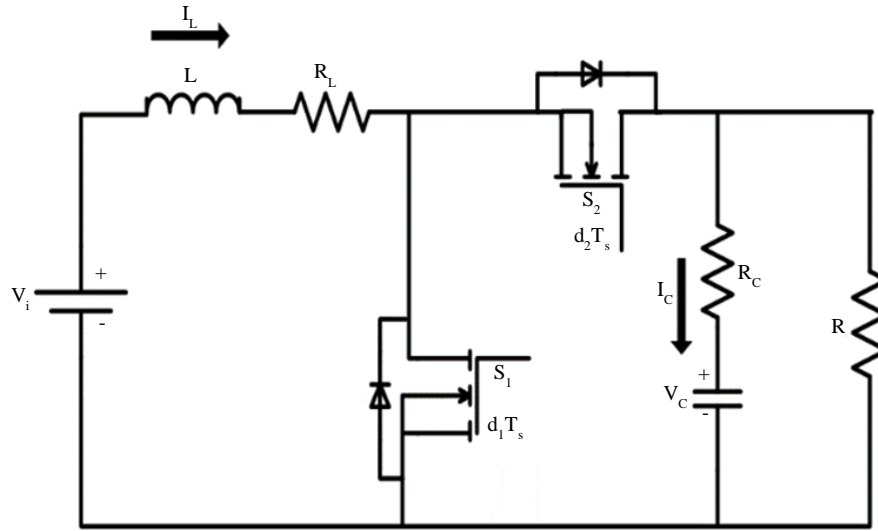


Fig. 3 Implemented bidirectional DC-DC converter

2.3. Energy Hub System

Microgrids require power compensation systems due to the inconsistent nature of renewable energy sources and changing demands.

These systems serve two purposes: first, to serve as a power source when microgrid generation falls short of meeting load demand, and second, to serve as a power sink when generation is at an excess.

While traditional battery storage is one compensation method, its slow dynamic response is insufficient for rapid load or renewable power changes.

In contrast, Supercapacitors (SCap) offer advantages such as quick response time and high instantaneous output power. Previous studies have highlighted the benefits of utilizing supercapacitors in various components of microgrids [15]. The suggested design aims to integrate Energy Hubs into the microgrid system for two primary purposes. Firstly, the supercapacitor absorbs strong transients

to ensure smooth power delivery during peak demand. Secondly, to maintain bus voltage, the battery system is employed.

Power regulation and balancing in microgrids are typically managed through generation unit outputs, such as PV units. However, generation units must operate at their maximum capacity during peak demand periods, which can be challenging.

Introducing an Energy Hub can take the pressure off the generation units and transfer control to other parts of the system, making it more efficient and reliable.

As shown in Figure 4, the energy hub is composed of a SCap coupled to a similar DC bus using bidirectional converters. The SCap control employs a cascaded PI system with an external voltage loop and an internal current loop, whereas battery control controls the bus voltage. The supercapacitor control ensures the isc value is zero during the steady state.

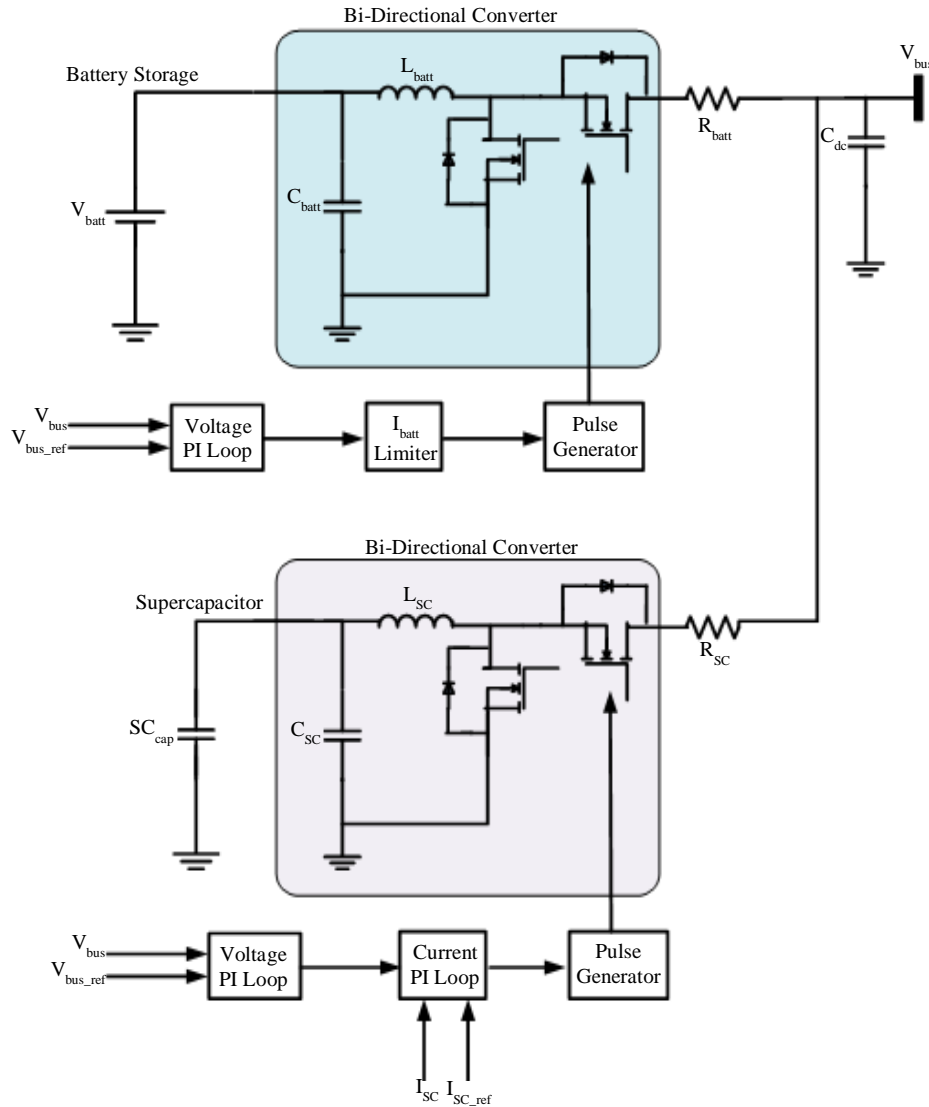


Fig. 4 Implemented energy hub system

2.4. About Charging Station of Electric Vehicles

Integrating vehicle-to-grid technology into microgrids has opened up new possibilities for transferring the compensation load to electric vehicles connected to charging stations. The benefits and challenges of adopting this technology have been thoroughly analyzed in previous studies [16]. The bus is linked to the charging station within the microgrid being examined. Its primary role is to recharge the Electric Vehicles (EVs) connected to it. Nevertheless, the EVs may also be used as an energy source to regulate the electrical grid during ultimate demand. The DC voltage at the bus is adjusted by altering the value of V_{ev} , which occurs when several EVs connect or disconnect from the charging station node, as depicted in Figure 5.

3. Proposed Control Technique

This article aims to present a method of energy optimization in a DC decentralized power network using a

distributed control technique. This approach does not rely on a communication network. Instead, power flow from individual sources is regulated through interconnected DC/DC converters.

3.1. Conventional Droop Control

The progress in power electronics has enabled decentralised microgrid systems' cost-effective and widespread implementation. A distributed control strategy can be effectively employed in microgrids, particularly at the regional level.

However, the regional controller must heavily rely on regional variables, which become vital to the control system to achieve this. Droop control is a non-feedback method of parallel control that does not require additional wiring for data transfer. This technique is widely adopted for its capacity to offer equilibrium in voltage and current

regulation. It relies on the fundamental droop control method to reduce the DC voltage by the output current [17]. The entire droop control method is expressed as follows:

$$V_{dck} = V_{dc}^* - I_{dck}R_{dk} \quad (14)$$

Where output voltage produced by separately converter's output can be described as V_{dck} , V_{dc}^* is the reference output voltage, the DC output current I_{dck} , the imaginary resistance R_{dk} and $k=1,2,3\dots$. Nonetheless, the effectiveness of this correlation is influenced by voltage deviations and imbalanced line losses, which prevent it from achieving optimal system performance. Due to better communication and quick data transmission among

converters, the distributed control technique can perform adaptive droop control at the secondary and primary control levels.

This approach enables gradual adjustment of the droop coefficient under varying load conditions. Voltage and current regulators are incorporated to provide voltage and impedance correction terms [18].

However, the automatic range of droop resistance may not always produce the desired outcome. To address this issue, a droop index approach has been utilized to fine-tune the droop resistance in real time, enhancing the performance of the droop mechanism.

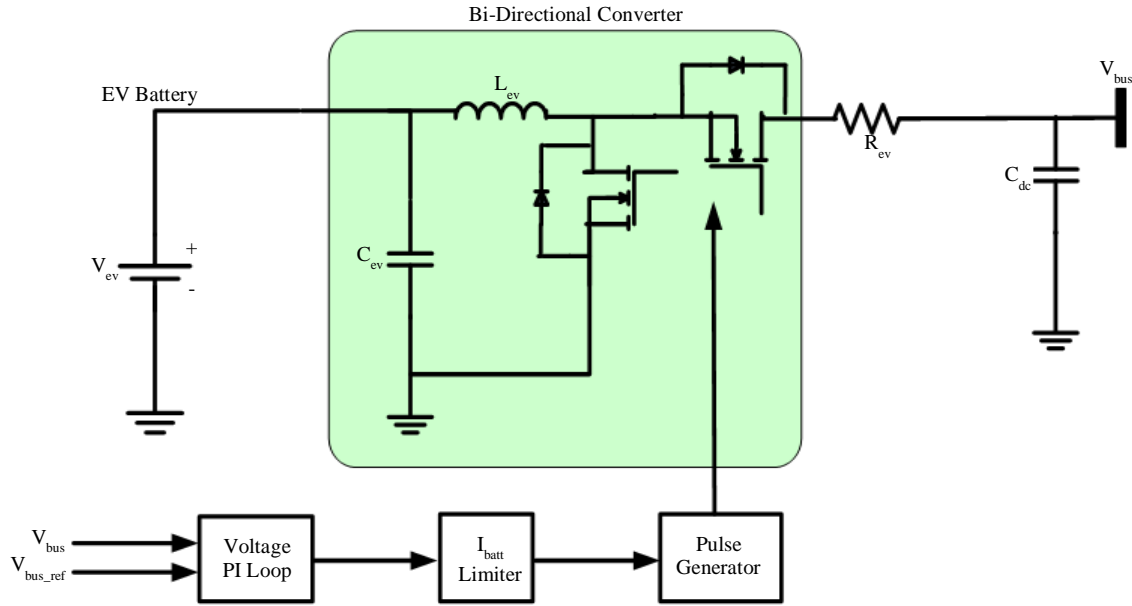


Fig. 5 Implemented EV charging station system

3.2. PI Controller

The PI controller generates the necessary duty cycle based on the output error, similar to the PID controller. In contrast, the PI controller is considerably less susceptible to such disruptions and produces an oscillation-free duty cycle. Moreover, the PI controller outperforms the PI controller concerning offset and steady-state error [19]. Therefore, considering all these factors, this paper utilizes a PI rather than a PID controller. The PI controller's mathematical representation is seen in the equation below.

$$u(t) = K_i \int_0^t e(t) dt + K_p e(t) \quad (15)$$

The $e(t)$ error signal represents the disparity between the bus value and the reference signals, Voltage (V_{bus}) and reference voltage (V_{bus_ref}).

$$e(t) = V_{bus} - V_{bus_ref} \quad (16)$$

The dual-loop control technique entails the utilization of two PI controllers: one for the voltage loop and the second for the current loop. The initial controller directly receives feedback from the converter's output, and its output is subsequently conveyed to the following controller, responsible for generating the requisite duty cycle, as shown in Figure 6, with parameters shown in Table 1.

When converter characteristics such as the voltage at the input and current at the output are affected by nonlinear or continually changing circumstances and output filter performance, tuning the PI controller becomes cumbersome and time-consuming.

In addition, conventional PI tuning lacks a right-half plane zero, resulting in a limited understanding of the converter's behaviour. This can lead to an over-damped output voltage for boost converters [20]. To address these drawbacks, this paper employs an ANN controller.

Table 1. PI control parameters

Mode	K_{pv}	K_{iv}	K_{pi}	K_{ii}
Battery	0.2	2.45	0.45	2.8
Supercapacitor	0.1	4	0.27	3.2
PV-Battery	0.1	4	10	4

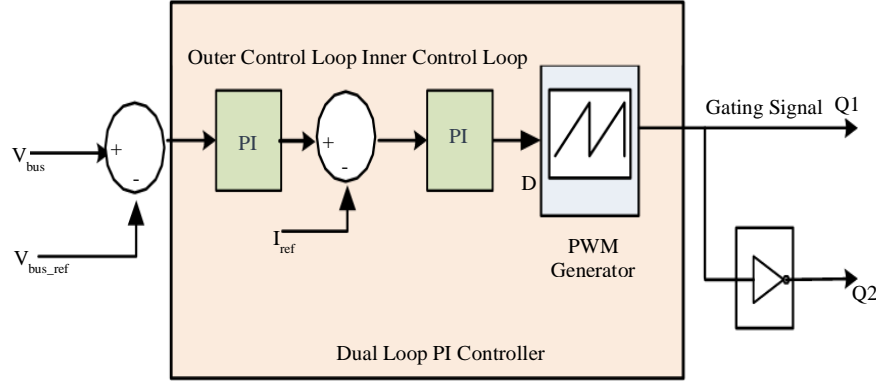


Fig. 6 Block diagram of a dual-loop PI controller

3.3. About ANN Controller

The lower portion of Figure 7 shows the suggested arrangement for the Artificial Neural Network controller. Its four levels comprise a hidden layer, a pair of visible layers, and a layer of output. The value of the error term and the value of the integral of the error term are the two inputs the controller receives.

$$e_{V_c}(k) = v_{bus}(k) - v_{bus_ref}^*(k) \tag{17}$$

$$S_{V_c}(k) = \int_0^k e_{V_c}(t) dt \tag{18}$$

Where $v_{bus}(k)$ is the DC bus voltage, $v_{bus_ref}^*(k)$ is the voltage shown by (17) reference, (18) It is worth noting that the ANN regulate input signals, just like the classic PI controllers, are the error terms and integrals of error.

The calculation $v_A^*(k)$ is created as the controller’s output from the output layer. $v_A^*(k)$ The normalized signal necessitates a PWM gain for the switching power converter to achieve the converter control signal $v_A(k)$, given by:

$$v_A(k) = k_{PWM} A(e_{V_c}(k), S_{V_c}(k), \vec{w}) \tag{19}$$

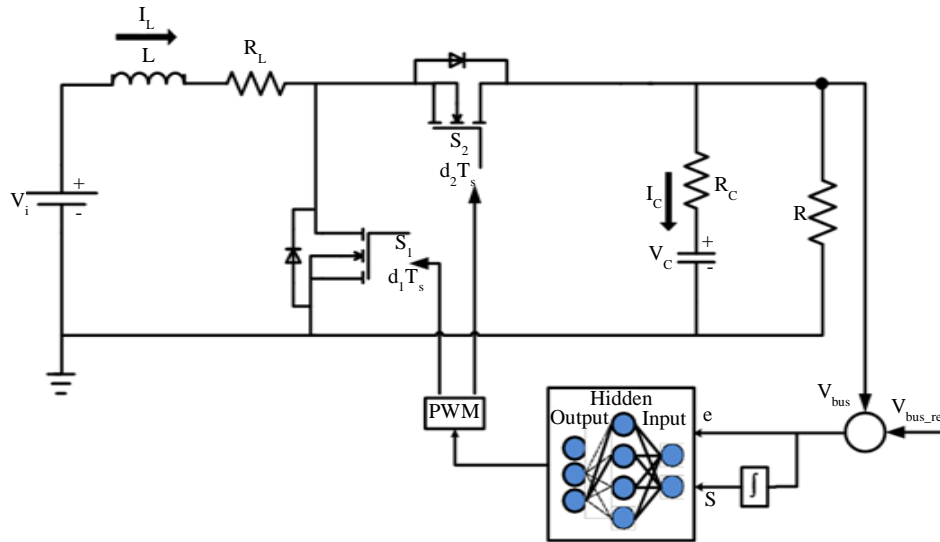


Fig. 7 An independent DC/DC converter under ANN control with loads

3.3.1. Training ANN Controller

To achieve optimal performance, the ANN controller needs to undergo training through Approximation Dynamic Programming (ADP) [21]. In the context of the DC microgrid application, the estimated dynamic programming cost-to-go function is as follows:

$$C(v_c) = \sum_{k=1}^N [v_{bus}(k) - \int v_{bus_{ref}}^*(k)]^2 \quad (20)$$

To achieve optimum control, the ANN controller must minimize the cost-to-go function (20) during training using Approximation Dynamic Programming (ADP). Since the output of the converter is used as feedback for the network’s input at the next time step, the ANN is a recurrent network in a closed-loop control.

To train the recurrent network, the weight vector must be calculated using the gradient of the cost-to-go function (20). $\frac{\partial C}{\partial \vec{w}}$ Similarly to the chain rule, the ANN is trained using the Levenberg-Marquardt (LM) algorithm once the inputs are acquired, and the Jacobian matrix is calculated using the Forward Accumulation Through Time (FATT) algorithm. The cost-to-go function (20) is then computed using Equations (17), (18), and (19) starting from the obtained inputs. A more detailed explanation of the training process can be found. Finally, the ANN weights are updated to modify the network’s weights after each training epoch $\Delta \vec{w}$ the network’s weights may be limited by acquiring a training epoch.

$$\vec{w}_{update} = \vec{w} + \Delta \vec{w} \quad (21)$$

The operation may be interrupted after it fulfils a requirement. Repeated network weight adjustments are made to reduce the impact of the ADP cost-to-go function (20). Following a successful training phase, an ANN based on ADP optimizes the bus voltage and can track the reference voltage. Figure 8 and Figure 9 below show the block diagram

of Artificial Neural Network and ANN training results, respectively. Training an ANN in MATLAB Simulink can be accomplished by following these steps:

- Define the ANN architecture: Determine the network’s structure, specifying the number of layers, neurons, activation functions, and interconnections between neurons.
- Prepare the training data: Assemble a labelled dataset for network training, ensuring it is partitioned into training, validation, and testing subsets.
- Configure the training algorithm: Choose an appropriate training algorithm for optimizing network weights during training. MATLAB Simulink offers a range of built-in algorithms, including backpropagation, resilient backpropagation, and Levenberg-Marquardt. In this case, the Levenberg-Marquardt training algorithm is employed.
- Model the neural network in Simulink: Develop a representation of the neural network architecture using Simulink’s Neural Network Toolbox.
- Set up the training environment: Adjust training parameters, such as the number of epochs, learning rate, momentum, and error tolerance, to optimize the training process.
- Train the network: Execute the Simulink model to train the network with the designated training dataset. Monitor training progress by tracking the training and validation errors.
- Evaluate the trained network: Employ the testing dataset to assess the trained network’s performance post-training.
- Deploy the network: Employ the trained network to make predictions or classify new data. MATLAB Simulink provides a comprehensive array of tools and functions for training, validating, and testing artificial neural networks. Furthermore, a wealth of online resources offers tutorials and examples on how to train ANNs using MATLAB Simulink.

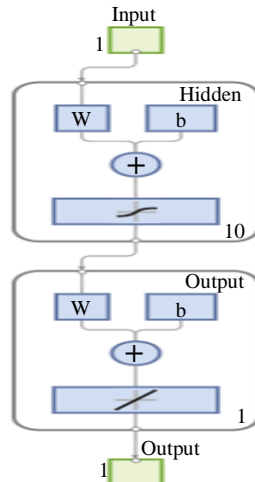


Fig. 8 Block diagram of Artificial Neural Network

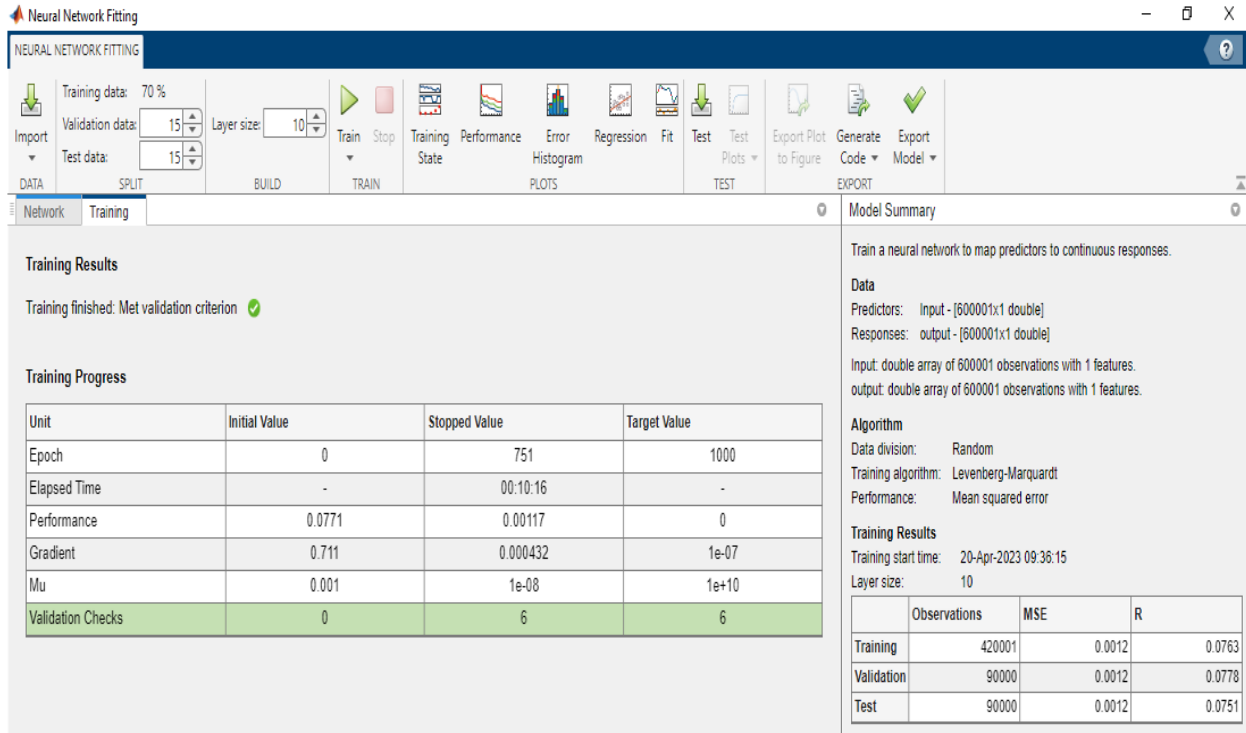


Fig. 9 Artificial Neural Network training result in MATLAB Simulink

4. Discussion of Simulation Results

The suggested control strategy underwent a comprehensive evaluation to assess its capacity to effectively and precisely manage bus voltage while optimizing load distribution.

Moreover, it was subjected to rigorous testing across various scenarios to test its resilience and adaptability. For in-depth insights into the results of each of these tests, the subsequent sections, where detailed descriptions are provided.

4.1. Dynamic Load Changes

The efficacy of the suggested power management system was assessed for sudden changes in load characterized by a rapid increase and subsequent decline, as well as in comparison to the droop controller, PI controller, and ANN controller.

During these tests, regional controllers employed specific control algorithms to counteract bus voltage fluctuations. As power generation decreased, the Energy Hub introduced power into the microgrid, with the supercapacitor handling abrupt power transients until the batteries could achieve the new steady-state value. The outcomes are depicted in Figure 10 indicate that the proposed ANN control approach handles sudden changes in load proficiently, ensuring effective bus voltage and power regulation. The droop controller revealed the most significant bus voltage deviation.

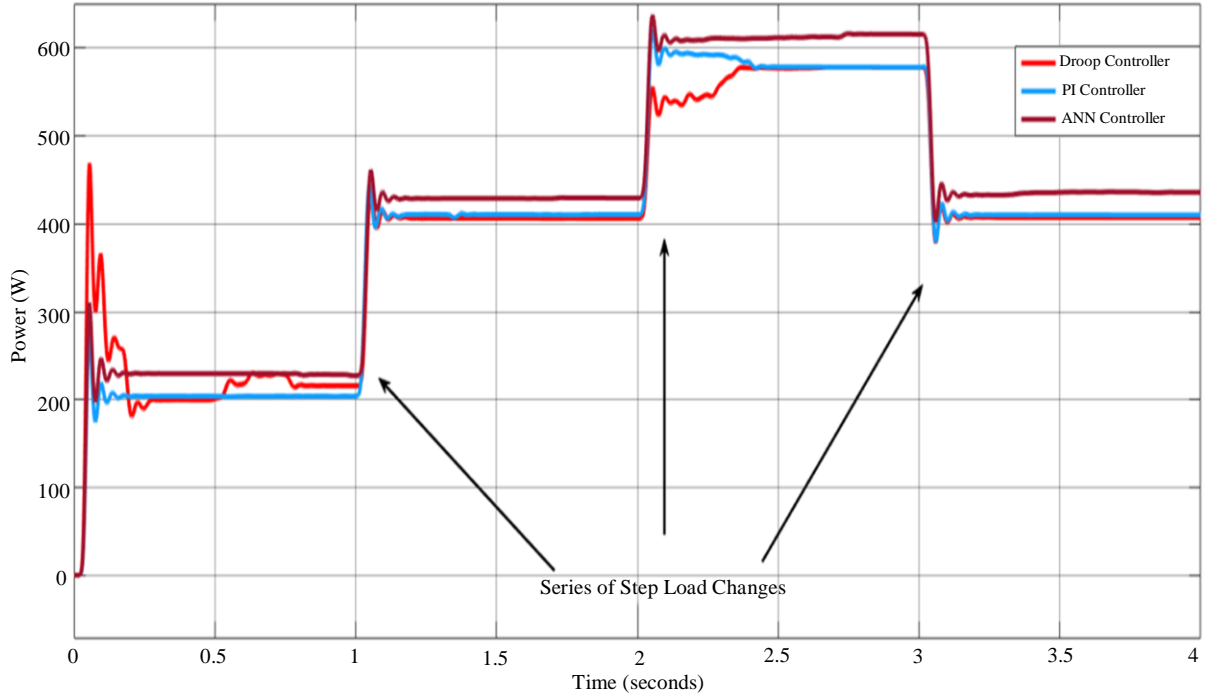
4.2. Communication Delay

The control method proposed in this study was tested for its ability to respond to controller communication delays in a distributed microgrid mode. A 200 ms communication latency was imposed between each district controller in the system, and the strategy was simulated.

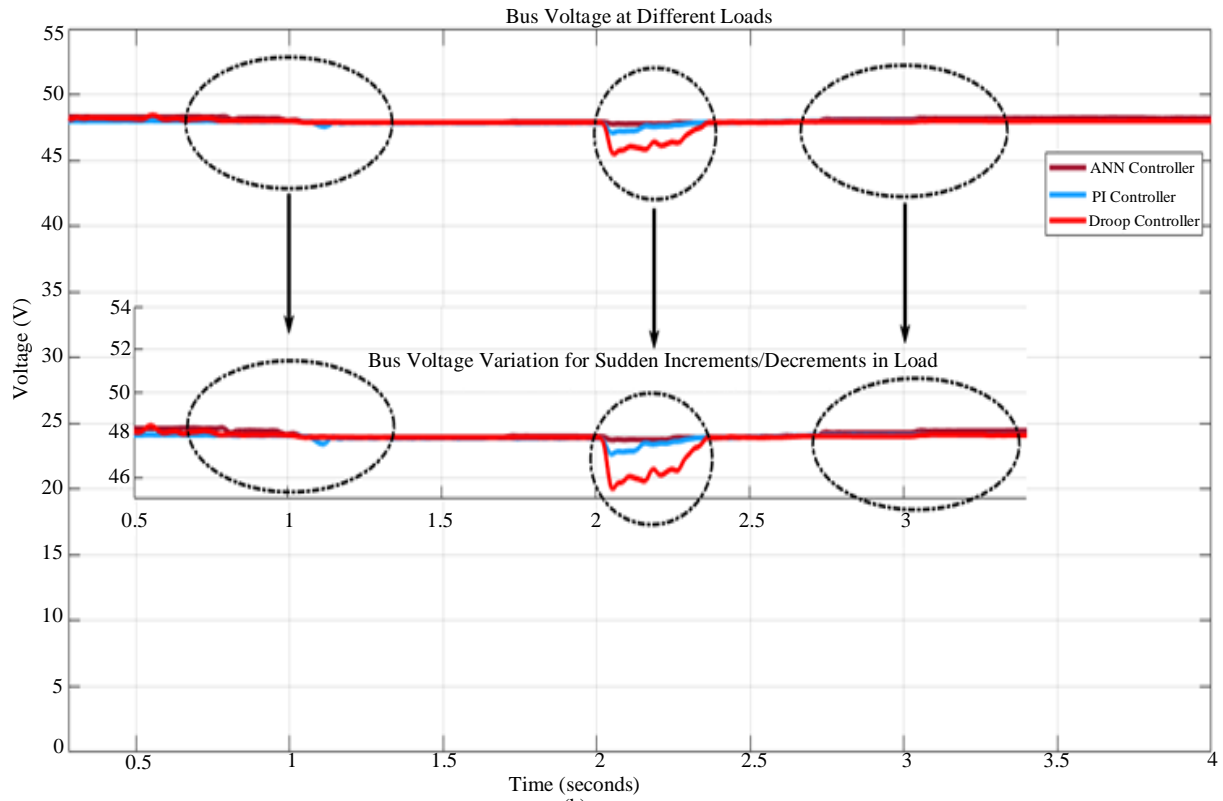
The results are presented in Figure 11, where the suggested ANN control method demonstrates faster voltage stabilization, with a voltage stabilization time of 0.15 s. The voltage variance is higher with droop control than with PI and ANN controllers, but it quickly dissipates with the ANN controller. This suggests that the projected power can stabilize bus voltage even if there is a communication delay between the regional controllers due to the distributed mode.

4.3. PV Battery Storage Node Simulation

The simulation results indicate that a decrease in solar irradiation reduces the battery's charging current, and the opposite happens when solar irradiation increases. The Photovoltaic (PV) system is prioritised over the battery; when the battery is ultimately charged, the PV operates in low-power mode. The InC algorithm extracts the most electricity from the PV system. The PV-battery node was subjected to various simulations to assess its performance under different conditions like sudden changes in irradiance (250-1000 W/m²), abrupt decreases in irradiance (1000-250 W/m²), unexpected variations in load, and temperature fluctuations. The simulation results for each of these scenarios are presented in Figure 12.



(a)



(b)

Fig. 10 Step-load change in (a) Power, and (b) Voltage.

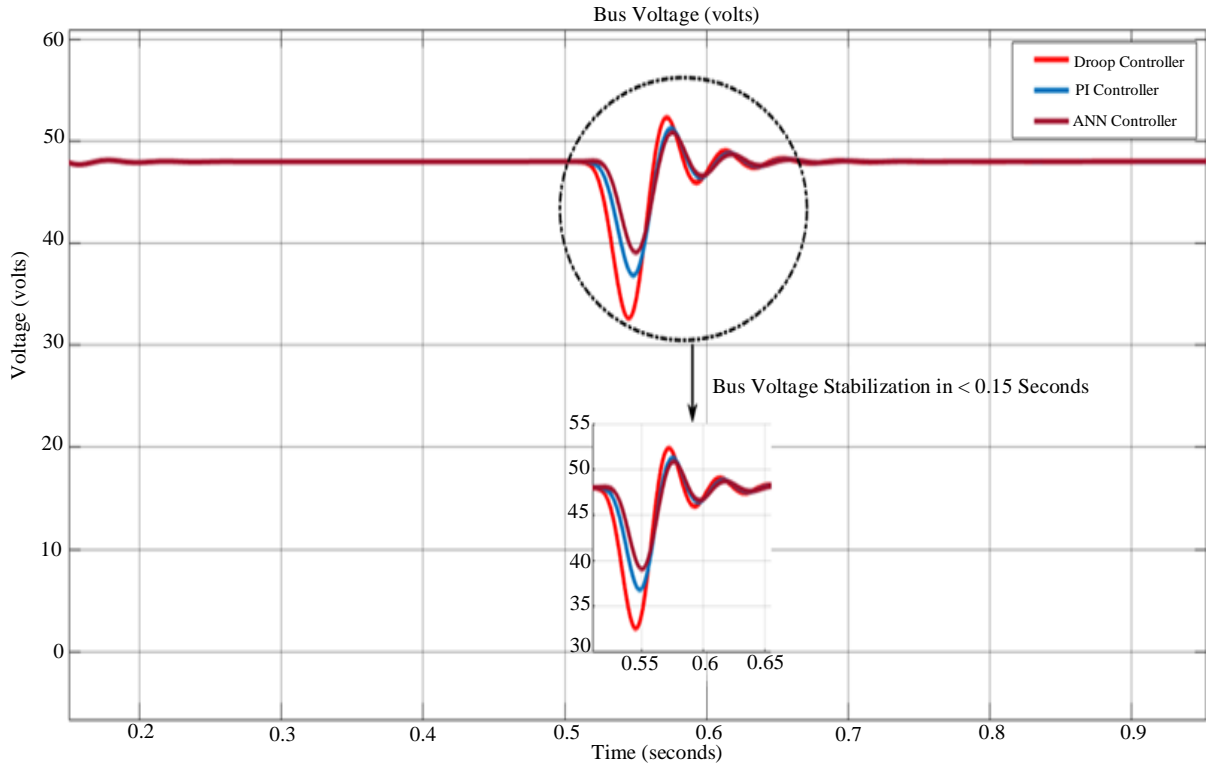


Fig. 11 Simulation with a communication latency of 200 milliseconds

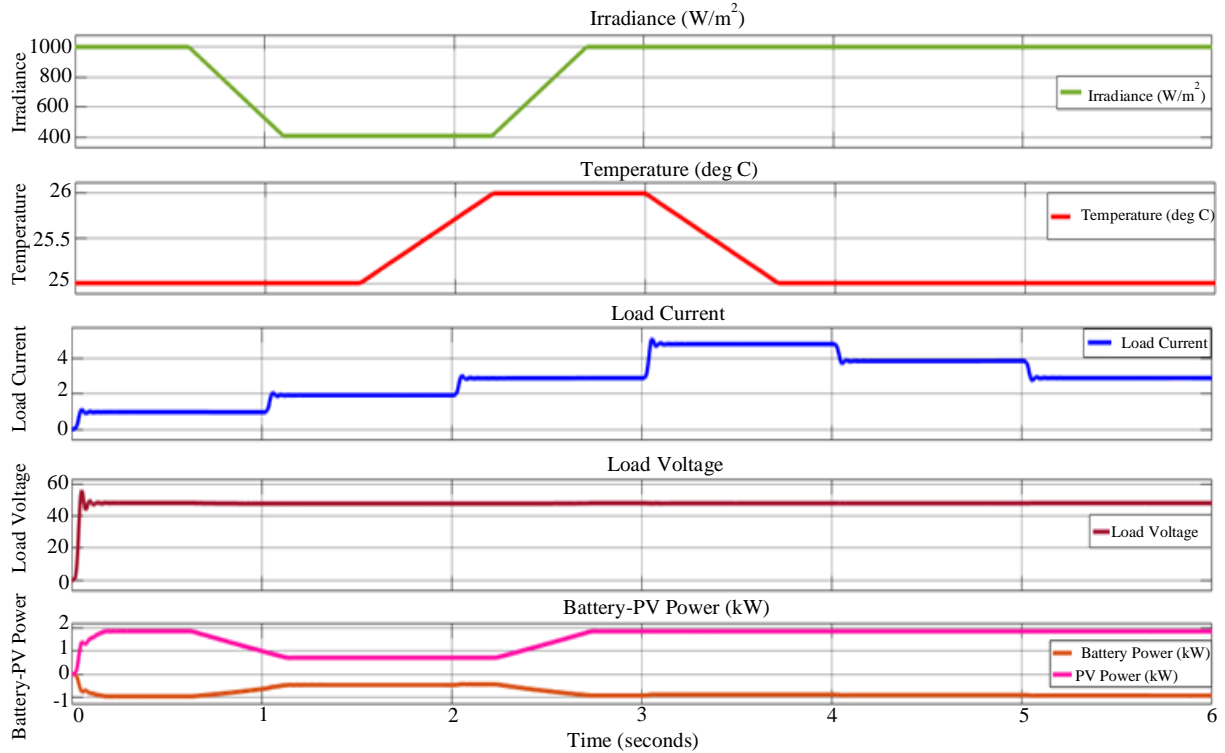


Fig. 12 Results of simulation for the PV and battery system

5. Conclusions

Controlling voltage stability in a standalone DC microgrid can be challenging, and this study aims to investigate a controller for regulating DC/DC converters and compare it with other control methods. The system's performance was evaluated, and it was found that the suggested approach can successfully control the bus voltage

to the chosen level and regulate the converter output power quickly when the load changes. According to the findings, the proposed approach could successfully maintain voltage stability in a DC microgrid. The ANN controller's performance is also analyzed in various transient conditions, including quickly tracking voltage references and tolerating load fluctuations.

References

- [1] Parag Jose Chacko, and Meikandasivam Sachidanandam, "An Optimized Energy Management System for Vehicle to Vehicle Power Transfer Using Microgrid Charging Station Integrated Gridable Electric Vehicles," *Sustainable Energy, Grids and Networks*, vol. 26, 2021. [[CrossRef](#)] [[Google Scholar](#)] [[Publisher Link](#)]
- [2] Bingzhang Li, Shenghua Huang, and Xi Chen, "Performance Improvement for Two-Stage Single-Phase Grid-Connected Converters Using a Fast DC Bus Control Scheme and a Novel Synchronous Frame Current Controller," *Energies*, vol. 10, no. 3, pp. 1-30, 2017. [[CrossRef](#)] [[Google Scholar](#)] [[Publisher Link](#)]
- [3] Dezhi Xu et al., "A Novel Adaptive Neural Network Constrained Control for a Multi-Area Interconnected Power System with Hybrid Energy Storage," *IEEE Transactions on Industrial Electronics*, vol. 65, no. 8, pp. 6625-6634, 2018. [[CrossRef](#)] [[Google Scholar](#)] [[Publisher Link](#)]
- [4] Anand K. Singh, Suraj A. Dahat, and Chetan W. Jadhao, "High Step-up DC/DC Converters Topologies," *International Journal of Recent Engineering Science*, vol. 5, no. 2, pp. 1-3, 2018. [[CrossRef](#)] [[Publisher Link](#)]
- [5] Srinivas Punna, Rupesh Mailugundla, and Surender Reddy Salkuti, "Design, Analysis and Implementation of Bidirectional DC-DC Converters for HESS in DC Microgrid Applications," *Smart Cities*, vol. 5, no. 2, pp. 433-454, 2022. [[CrossRef](#)] [[Google Scholar](#)] [[Publisher Link](#)]
- [6] Nikhil Korada, and Mahesh K. Mishra, "Grid Adaptive Power Management Strategy for an Integrated Microgrid with Hybrid Energy Storage," *IEEE Transactions on Industrial Electronics*, vol. 64, no. 4, pp. 2884-2892, 2017. [[CrossRef](#)] [[Google Scholar](#)] [[Publisher Link](#)]
- [7] Yang Gao, and Qian Ai, "Distributed Cooperative Optimal Control Architecture for AC Microgrid with Renewable Generation and Storage," *International Journal of Electrical Power & Energy Systems*, vol. 96, pp. 324-334, 2018. [[CrossRef](#)] [[Google Scholar](#)] [[Publisher Link](#)]
- [8] Xialin Li et al., "Observer-Based DC Voltage Droop and Current Feedforward Control of a DC Microgrid," *IEEE Transactions on Smart Grid*, vol. 9, no. 5, pp. 5207-5216, 2018. [[CrossRef](#)] [[Google Scholar](#)] [[Publisher Link](#)]
- [9] Yuyang Li et al., "A Virtual Inertia-Based Power Feedforward Control Strategy for an Energy Router in a Direct Current Microgrid Application," *Energies*, vol. 12, no. 3, pp. 1-14, 2019. [[CrossRef](#)] [[Google Scholar](#)] [[Publisher Link](#)]
- [10] Wensheng Song, Nie Hou, and Mingyi Wu, "Virtual Direct Power Control Scheme of Dual Active Bridge DC-DC Converters for Fast Dynamic Response," *IEEE Transactions on Power Electronics*, vol. 33, no. 2, pp. 1750-1759, 2018. [[CrossRef](#)] [[Google Scholar](#)] [[Publisher Link](#)]
- [11] Oladimeji Ibrahim et al., "Development of Observer State Output Feedback for Phase-Shifted Full Bridge DC-DC Converter Control," *IEEE Access*, vol. 5, pp. 18143-18154, 2017. [[CrossRef](#)] [[Google Scholar](#)] [[Publisher Link](#)]
- [12] Guanghui Sun, and Zhiqiang Ma, "Practical Tracking Control of Linear Motor with Adaptive Fractional Order Terminal Sliding Mode Control," *IEEE/ASME Transactions on Mechatronics*, vol. 22, no. 6, pp. 2643-2653, 2017. [[CrossRef](#)] [[Google Scholar](#)] [[Publisher Link](#)]
- [13] Saurabh S. Shingare, Prabodh Khampariya, and Shashikant Bakre, "Application of ANN-Based Approach for Fault Location in Extra High Voltage Networks," *International Journal of Engineering Trends and Technology*, vol. 71, no. 2, pp. 440-449, 2023. [[CrossRef](#)] [[Publisher Link](#)]
- [14] Yunfei Yin et al., "Observer-Based Adaptive Sliding Mode Control of NPC Converters: An RBF Neural Network Approach," *IEEE Transactions on Power Electronics*, vol. 34, no. 4, pp. 3831-3841, 2019. [[CrossRef](#)] [[Google Scholar](#)] [[Publisher Link](#)]
- [15] Yabin Gao et al., "Distributed Soft Fault Detection for Interval Type-2 Fuzzy-Model-Based Stochastic Systems with Wireless Sensor Networks," *IEEE Transactions on Industrial Informatics*, vol. 15, no. 1, pp. 334-347, 2019. [[CrossRef](#)] [[Google Scholar](#)] [[Publisher Link](#)]
- [16] Zhenyu Zhu et al., "Improved T-S Fuzzy Control for Uncertain Time-Delay Coronary Artery System," *Complexity*, vol. 2019, pp. 1-11, 2019. [[CrossRef](#)] [[Google Scholar](#)] [[Publisher Link](#)]
- [17] Abhishek Kumar Gupta, and Ravi Saxena, "Review on Widely-Used MPPT Techniques for PV Applications," *2016 International Conference on Innovation and Challenges in Cyber Security (ICICCS-INBUSH)*, Noida, India, pp. 270-273, 2016. [[CrossRef](#)] [[Google Scholar](#)] [[Publisher Link](#)]

- [18] Ayesha Firdaus, and Sukumar Mishra, “Auxiliary Signal-Assisted Droop-Based Secondary Frequency Control of Inverter-Based PV Microgrids for Improvement in Power Sharing and System Stability,” *IET Renewable Power Generation*, vol. 13, no. 13, pp. 2328-2337, 2019. [[CrossRef](#)] [[Google Scholar](#)] [[Publisher Link](#)]
- [19] Vahid MortezaPour, and Hamid Lesani, “Adaptive Primary Droop Control for Islanded Operation of Hybrid AC-DC MGs,” *IET Generation, Transmission & Distribution*, vol. 12, no. 10, pp. 2388-2396, 2018. [[CrossRef](#)] [[Google Scholar](#)] [[Publisher Link](#)]
- [20] Ranjan Pramanik, and B.B. Pati, “Modelling and Control of a Non-Isolated Half-Bridge Bidirectional DC-DC Converter with an Energy Management Topology Applicable with EV/HEV,” *Journal of King Saud University - Engineering Sciences*, vol. 35, no. 2, pp. 116-122, 2023. [[CrossRef](#)] [[Google Scholar](#)] [[Publisher Link](#)]
- [21] Weizhen Dong et al., “Control of a Buck DC/DC Converter Using Approximate Dynamic Programming and Artificial Neural Networks,” *IEEE Transactions on Circuits and Systems I: Regular Papers*, vol. 68, no. 4, pp. 1760-1768, 2021. [[CrossRef](#)] [[Google Scholar](#)] [[Publisher Link](#)]